Interannual relationship between intensity of rainfall intraseasonal oscillation and summer-mean rainfall over Yangtze River Basin in eastern China

Yanjun Qi[1] · Tim Li[2] · Renhe Zhang[3] · Yang Chen[1]

Abstract

The analysis of observational rainfall shows that the intensity of rainfall intraseasonal oscillation (ISO) and the summer-mean rainfall over the middle-lower reaches of the Yangtze River Basin (YRB) exhibit a significant positive correlation during 1979–2007. A stronger (weaker) ISO variability is often associated with wet (dry) summer in the YRB. The composite ISOs in both the wet and dry summers are further analyzed. In the wet summers, the rainfall ISO in YRB is primarily associated with the northward propagation of a low-level cyclone-anticyclone pair from the tropics. Cyclonic vorticity and associated boundary layer convergence strengthen the rainfall in situ. In contrast, the rainfall ISO in YRB in the dry summers is primarily associated with the westward propagation of an anomalous anticyclone. Southerly flow to the west of the anomalous anticyclone enhances rainfall in YRB through anomalous moisture advection. In addition to the difference in ISO propagation, the background mean state also shows a marked difference. The diagnosis of water vapor flux budget shows that the convergence and advection of seasonal mean moisture play a critical role in maintenance of the intraseasonal rainfall in the YRB. A greater mean ascending motion and associated higher mean moisture in YRB in the wet summers favor greater intraseasonal rainfall variability in situ. The mean state difference is responsible for distinctive vertical structures of boundary layer vertical velocity. A possible feedback of the ISO to the summer-mean rainfall over the YRB is also discussed.

Keywords Intraseasonal oscillation · Summer rainfall · Yangtze River Basin

1 Introduction

The abnormal Asian summer monsoon associated with active/break monsoon cycles influence significantly the climate, agriculture and people societal activities. Previous studies exhibited that the prolonged rainy/dry episode, which will result in severe flooding/drought and extreme temperature events, is closely related to the phase evolution of boreal summer intraseasonal oscillation (BSISO) (Annamalai and

Slingo 2001; Li 2014; Lee et al. 2013; Diao et al. 2018). As a component part of Asian summer monsoon, the East Asian summer monsoon (EASM) is usually referred to both the tropical and subtropical monsoons, encompassing a large area spanning the equatorial regions of Southeast Asia, the South China Sea (SCS), and the subtropical region extending from eastern China to Korea and Japan (Lau et al. 1988; Chen et al. 2000). The commencement of subtropical EASM is characterized by a sudden change from relatively dry condition over the Yangtze River Basin (YRB) in eastern China to periods of continuous rain spells, which is called Meiyu in China or Baiu in Japan (Lau and Chan 1986). The alternative change of active/break cycles in summer rainfall in the middle-lower reaches of the YRB reflects the abrupt northward advance of the Meiyu front, which is a major convergence zone dominated in East China during the boreal summer (Tao and Chen 1987; Ding and Wang 2008). The prominent summer rainfall with a dual- or triple-peak mode in the YRB is directly modulated by the intraseasonal oscillation (ISO), which originates from the tropical region of SCS

✉ Yanjun Qi
qiyj@cma.gov.cn

1   State Key Laboratory of Severe Weather, Chinese Academy of Meteorological Sciences, Beijing, China

2   Department of Atmospheric Sciences, International Pacific Research Center, University of Hawaii at Manoa, Honolulu, USA

3   Department of Atmospheric and Oceanic Sciences & Institute of Atmospheric Sciences, Fudan University, Shanghai, China

and western north Pacific (WNP) and exhibits northward or northwestward propagation (Wang and Xu 1997; Hsu and Weng 2001; Jiang et al. 2004; Li and Wang 2005; Li 2010; Mao et al. 2010; Yang et al. 2010, 2014; Li et al. 2015; Oh and Ha 2015). The ISO is found to be related to not only the climatological summer rainfall but also the extreme rainfall and heat-wave events over eastern China (Zhang et al. 2009; Ren et al. 2013; Hus et al. 2015; Chen and Zhai 2017; Gao et al. 2017). Hus et al. (2016) investigated the impacts of boreal summer ISO on the probability and spatial distributions of extreme rainfall occurrence over southern China, suggesting a potential focus for monitoring and probabilistic prediction of extreme rainfall events in southern China.

More case studies have demonstrated that the persistent strong rainfall over the YRB during summer is usually accompanied with ISO activities. The severe floods during the summer of 1998, which happened in the YRB in eastern China, have been shown to be related to the pronounced northward propagation of ISO from the tropics and the southwestward propagation from mid- and high latitudes (Li et al. 2015). The two sources of intraseasonal variability from tropics and mid- to high latitudes converged in the YRB and resulted in the spells of rainfall (Chen et al. 2001). Based on phase composite analysis, it is found that the strong intraseasonal summer Yangtze-River rainfall was mainly contributed by the northwestward propagation of alternating cyclonic-anticyclonic anomalous circulation, which originated from the WNP. The low-level wind convergence toward the Yangtze River between northeasterlies associated with the anomalous cyclone and southwesterlies associated with the anomalous anticyclone provides favorable circulation condition for the strong precipitation in the YRB (Qi et al. 2016). In another flooding year of 1991 (Lu and Ding 1996), the Yangtze-Huai River suffered several devastating rainfall periods, indicating experienced strong ISOs. As suggested by Mao and Wu (2006), the intraseasonal variation of the Yangtze-River rainfall was related to the ISO atmospheric circulations, which exhibited coupled anomalous flow pattern between the lower and upper troposphere. Dynamically, the active and break sequences of rainfall in the YRB were controlled by the coupling intraseasonal circulations between the low-level relative vorticity and the upper-level divergence. During an abrupt drought-flood transition event occurred in the YRB in early summer of 2011, Yang et al. (2013) emphasized the importance of intraseasonal variability in triggering the strong rainfall from the point of meridional circulation of upper troposphere. In the individual years associated with heavy summer rainfall in eastern China, the ISO plays an important role in organizing and regulating summer rainfall in eastern China.

The summer rainfall in the YRB exhibits not only intraseasonal variation but also remarkable interannual variability. The prominent feature of interannual variation in summer-mean rainfall is characterized by the anomalous wet or dry season in eastern China. Simultaneously, the related intraseasonal variability with summer rainfall in eastern China also experiences significant year-to-year variation in its intensity and propagation character (Li and Li 1999). Thus it is speculated that there might exist some linkage between the summer rainfall and ISO. Most of previous studies emphasized the atmospheric ISO exhibits stronger activity over eastern China in wet summer years than in dry summer years (Li 1992; Yang and Li 2003), and less attention was paid to the statistical relationship between the summer-mean rainfall in eastern China and the ISO on interannual timescale. The objective of this study is to examine the linkage between the summer-mean rainfall and the intensity of ISO on the interannual timescale in eastern China, especially over the YRB. The temporal-spatial characteristics of structure and evolution of ISO associated with summer rainfall and 850 hPa circulations are investigated. Further, the two-way possible interactions between the mean state and ISO are discussed based on the interannual relationship.

The data and method used in this study are described in Sect. 2. The intraseasonal and interannual variations of summer precipitation in eastern China and its related with ISO characteristics in periodicity and intensity are presented in Sect. 3. In Sect. 4, the structure and evolution characteristics of ISO related to the summer rainfall and circulations in eastern China are described. In Sect. 5, the impacts of mean state on ISO rainfall are presented by the diagnosis of water vapor flux budget. In Sect. 6, the feedback of ISO perturbation to the summer rainfall is discussed. Finally, a summary and discussion is given in Sect. 7.

2 Data and methods

The daily gridded precipitation data of China with a resolution of 0.25°×0.25° is provided by the Information Center of China Meteorological Administration. This dataset is based on the daily rain gauge measurements at about 2400 stations of the Chinese national dense observational network, and integrated by using an optimal interpolation algorithm (Shen and Xiong 2015). To depict the ISO structure and evolution characteristics over eastern China, we adopt the high-resolution, gridded (0.5°×0.5°) daily precipitation dataset for the region of Monsoon Asia, which was compiled by the project of "Asian Precipitation-Highly Resolved Observational Data Integration Towards Evaluation of the Water Resources (APHRODITE's Water Resources)". The APHRODITE rainfall dataset was created primarily with a rain-gauge-observation data network using data collected from local meteorological/hydrological organizations by the Research Institute for Humanity and Nature (RIHN) and the Meteorological Research Institute (MRI) of the Japan Meteorological

Agency (JMA). The Monsoon Asia product (APHRODITE_ MA, hereinafter referred to as APHRO) used in this study covers the region of 60°–150°E, 15°S–55°N (Yatagai et al. 2012). In addition, daily-mean variables (including zonal wind *u* and meridional wind *v*, pressure vertical velocity *ω*, specific humidity as well as temperature) from the NCEP/ NCAR reanalysis with the resolution of 2.5° × 2.5° are used in this study. All datasets used in this study have the same record length from 1979 to 2007 (29 years). We consider May–August (MJJA) as the summer season in China.

The climatological daily-mean precipitation time series in the EASM region contains annual cycle and considerable fluctuations on intraseasonal timescale (Nakazawa 1992; Wang and Xu 1997). Therefore, the fast Fourier transform (FFT) is applied to the climatological daily-mean precipitation time series to extract the signals of intraseasonal variability. The standard deviation of the filtered precipitation in MJJA is used to measure the intensity of ISO. A Student *t* test is applied to test the significance of composite and correlation patterns.

3 Intraseasonal feature of summer precipitation in eastern China

The spatial distribution of summer precipitation in mainland China shows significant inhomogeneous feature with the maximum centers located in southern and eastern China. The summer precipitation in China decreases inland from the coastal region of southeast to northwest due to the impact of tropical monsoon, forming a slant rainfall pattern oriented in southwest-northeast direction (Fig. 1a). The western and northwestern parts of China receive less precipitation and are the typical dry regions in summer. The southern and eastern areas in China are the

key regions that explain more than 50% of summer precipitation. Besides the interannual variation, the summer precipitation in southern and eastern China experiences significant intra-seasonal variability. Figure 1b shows the standard deviation of rain rate in summer from May to August averaged for the period of 1979–2007. The maximum variation center of summer precipitation is located south of 25°N in southern China. The climate in southern China exhibits a typical monsoon characteristic, and thus experiences the impact of northward propagation of tropical waves or typhoon activities originated from the WNP. Another variation center of summer precipitation occurs in the middle-lower reaches of the YRB in eastern China, which is a sensitive region suffering from severe floods or droughts frequently (Fig. 1b). The strong intraseasonal fluctuation in summer precipitation in the YRB may result in an extremely wet or dry season (for example severe floods in summer 1998 and droughts in summer 1981). Thus, the domain of 110°–120°E, 27°–32°N with a large summer variation in precipitation (shown as a rectangle in Fig. 1b) is taken as the key region to investigate the interannual and intraseasonal variations of summer rainfall in the YRB.

To identify the climatologically dominant periodicity of ISO in summer rainfall in eastern China, spectral analysis is applied to the 29-year (1979–2007) climatological daily-mean rainfall in the APHRO data. The first four Fourier harmonics, which denote the annual, semiannual and seasonal cycles, are removed before carrying out the spectral analysis. Figure 2 shows the power spectra of the rainfall in the YRB, which is the region of significant correlation in Fig. 1b, with the lines of 95% confidence levels and red noise spectra. It can be seen that the dominant ISO periodicity in the YRB is the frequency band of 30–90 days. The ISO periodicity that we focus in
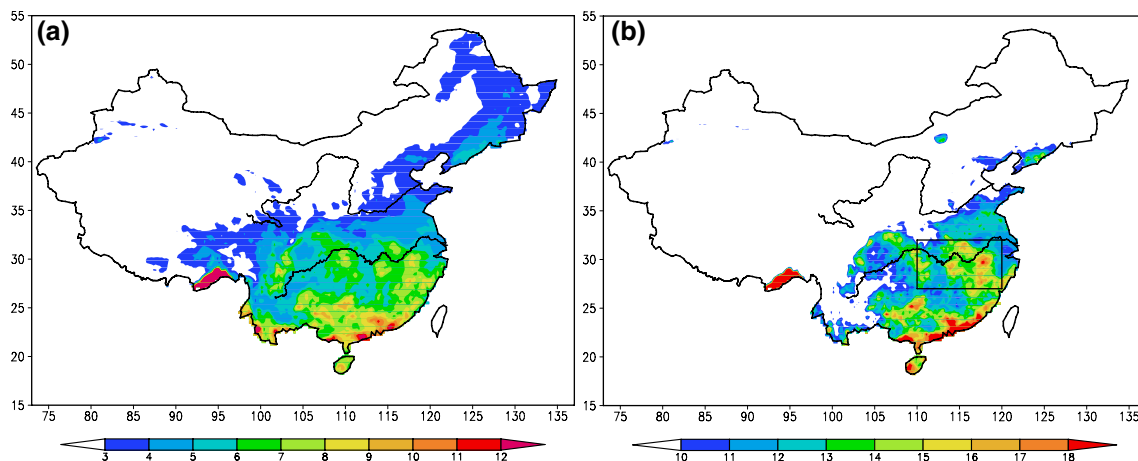

Fig. 1 a Distribution of daily rain rate during summer (MJJA) in 1979–2007 (unit: mm/day). **b** Averaged standard deviation of MJJA precipitation for the period of 1979–2007 (unit: mm/day)
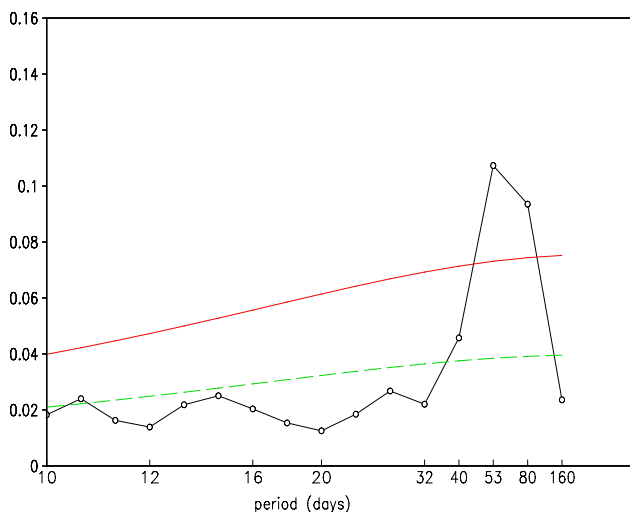
Fig. 2 Power spectrum (black curve with marked circle) of summer rainfall in the middle-lower reaches of the Yangtze River Basin (110°–120°E, 27°–32°N). Green dashed line indicates red noise spectrum, and red line indicates the 95% confidence level

this study is the 30–90 days band. Therefore, variables associated with ISO horizontal circulations and vertical structures in the following analysis and discussions are all filtered by 30–90 days band.

The overall intensity of summertime ISO is measured by the standard deviation of May–August intraseasonal rainfall anomalies. During the boreal summer, the maximum

variability centers are located along 15°N over the Bay of Bengal and the eastern Arabian Sea in the Indian monsoon region, and over the SCS and the Philippine Sea in the WNP sector. By using the land precipitation data, Fig. 3 displays the 29-yr mean (1979–2007) ISO intensity of May–August in APHRO. Besides the western part in India peninsula and the northern part of the Bay of Bengal, the large intraseasonal variability in China is located mainly in the southeastern part of China, especially along 30°N from the middle-lower reaches of the Yangtze River valley in China to the south of the Korea Peninsula and Japan. These regions with large intraseasonal variability are the locations of Meiyu front in China and Baiu front in Japan. It indicates that the summer precipitation anomaly of eastern China is closely related to the fluctuations of ISO over East Asia (Lau et al. 1988).

For convenience of investigating the interannual variation of summer precipitation in the YRB and its relationship with ISO activity, we define the time series of MJJA rainfall averaged over the box of (110°–120°E, 27°–32°N) as the YRB index (shown in Fig. 1b). The regression of summer time (May–August) ISO intensity onto the YRB index shows a significant positive correlation over eastern China along the middle-lower reaches of the Yangtze River (Fig. 4a). It indicates that the interannual variation of the summer rainfall anomaly in the YRB exhibits a strong in-phase relationship with the summer-time ISO intensity. Generally, the rainy (dry) summers are associated with strong (weak) ISO

Fig. 3 Averaged summertime 30–90 days ISO intensity for the period of 1979–2007 (unit: mm/day)
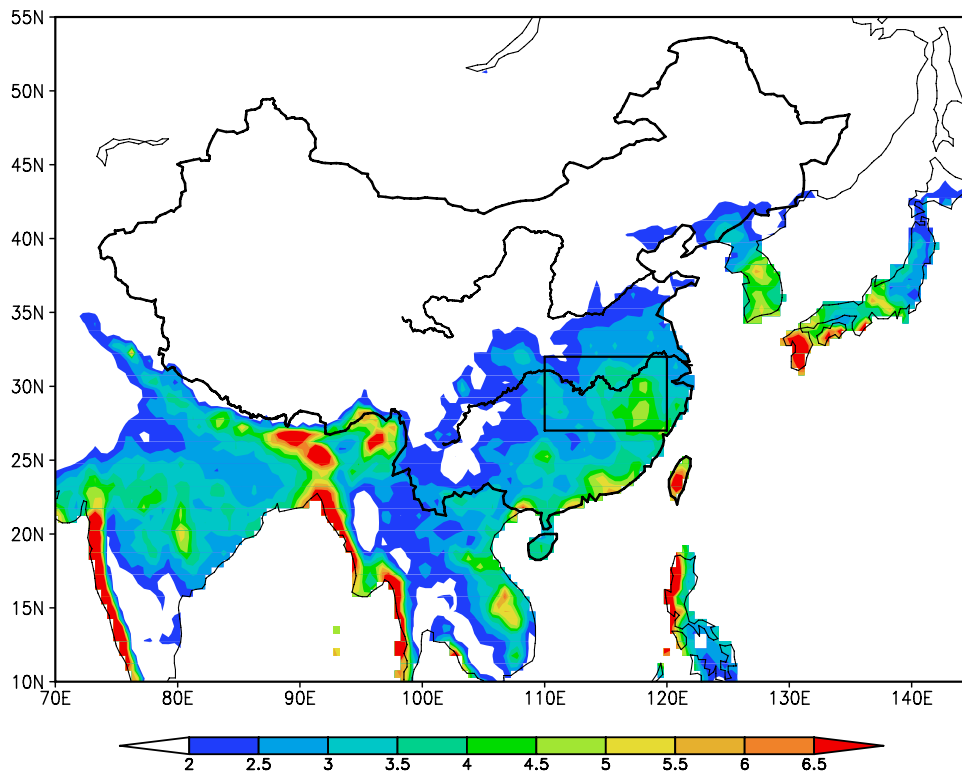
Fig. 4 Top: regression of summertime (MJJA) ISO intensity onto the YRB precipitation index for the period of 1979–2007. The regression correlation coefficients exceed the 95% significance level are shaded. Rectangle denotes the key region of the YRB. Bottom: standardized time series for standard deviation anomaly of the 30–90 days filtered rainfall (red) and summer-mean precipitation averaged over the YRB (green)
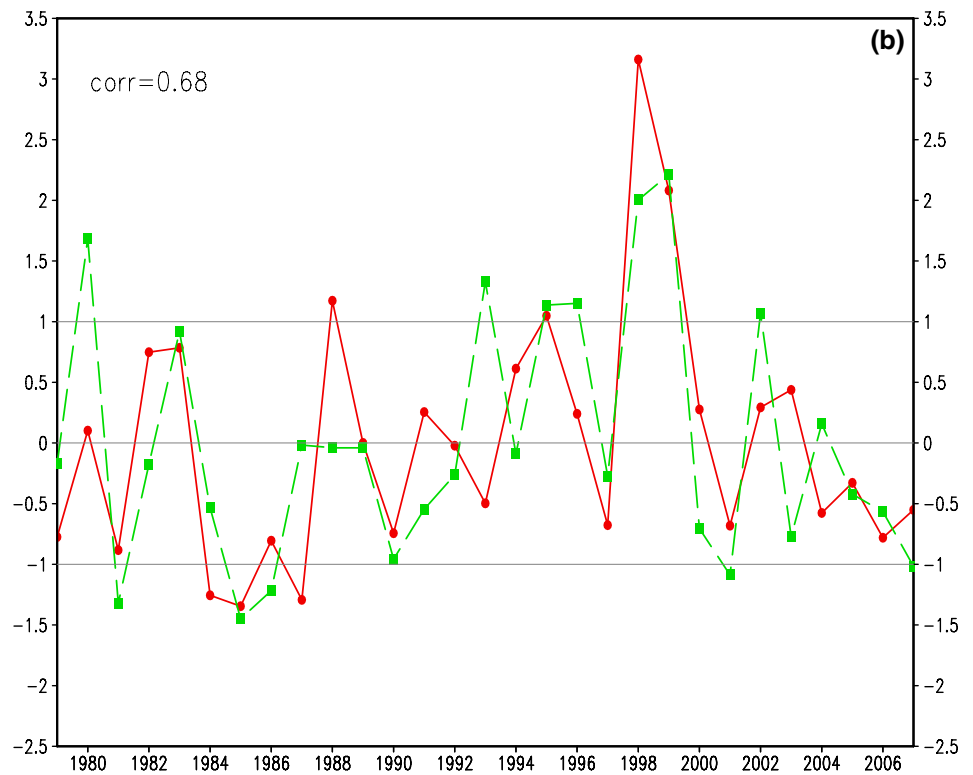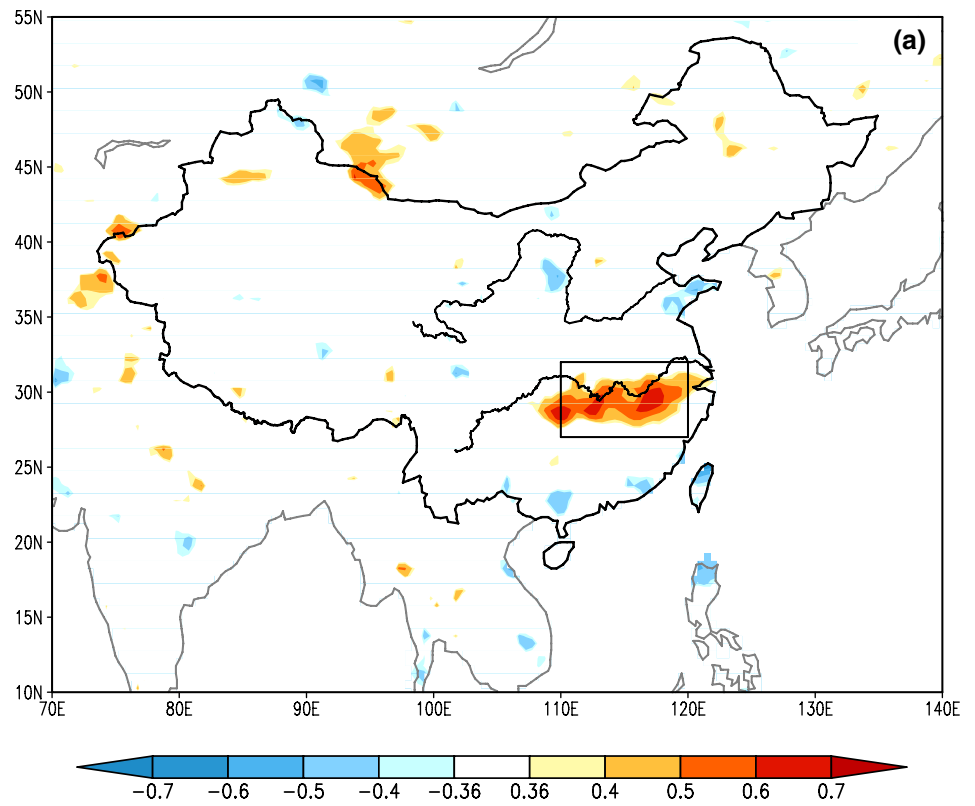
activities over the YRB. This relationship on the interannual timescale is quite different from the result of Qi et al. (2008), which showed a significant negative correlation between the ISO intensity and Indian summer-monsoon rainfall over the Indian subcontinent.

To further examine the in-phase relation, the summertime ISO intensity over the positive-correlated region is calculated and shown in Fig. 4. Both the ISO intensity and the summer-mean rainfall exhibit strong interannual variations. The simultaneous correlation coefficient between the two time series of the YRB index and the ISO intensity is 0.68, indicating a high relationship between the summermean rainfall and ISO intensity over the YRB on the interannual timescale. Here, the YRB index in rainfall anomalies is used to classify the wet or dry summers for the period of 1979–2007, with the MJJA rainfall anomaly above 1 (less than −1) standard deviation as wet (dry) summer. There were seven wet (1980, 1993, 1995, 1996, 1998, 1999, and 2002) and six dry (1981, 1985, 1986, 1990, 2001, and 2007) summers, which are selected according to the above definitions.

4 Evolution of ISO structures

In this section, the evolutions of ISO rainfall and 850-hPa wind anomalies are investigated by compositing eight phases in the ISO cycle. For the seven wet and six dry summers, we construct the composite analysis using only those ISO cycles with amplitudes exceeding one (or negative one) standard deviation according to the time series of 30–90 days filtered MJJA rainfall in the YRB for each selected summer. In the 30–90 days filtered rainfall time series, the period from a negative peak to a positive peak and then to the next negative peak is regarded as an ISO cycle. Each selected ISO cycle is divided into eight consecutive phases. The first negative peak is defined as Phase 1, the negative-turning-to-positive is defined as Phase 3 and the positive peak is defined as Phase 5 (the definition is the same as that in Wang et al. 2006; Qi et al. 2013), namely, Phase 1 and Phase 5 correspond, respectively, to the minimum and maximum rainfall anomalies in the YRB. According to the above definition, a total of 17 cycles is identified, with 10 cycles in the wet summers and 7 cycles in the dry summers. The mean interval between two adjacent phases is about 5 days in both wet and dry summers.

4.1 Composite in wet summers

Figure 5 shows the composite evolutions of 30–90 days filtered anomalies in rainfall and 850-hPa winds in the wet summers. During the wet summers, negative rainfall anomalies are found to along 30°N extending from the mid-lower

Yangtze River to south of Japan in Phase 1 (Fig. 5, Phase_1), indicating that the region around the YRB is in the driest stage. The southern China is controlled by the northeasterlies in the lower troposphere, which lie northwest of the anomalous cyclonic circulation with the center over the SCS. From the height-phase cross section of the YRB region (Fig. 6), we can see negative vorticity and divergence anomalies in the low-level troposphere and positive vorticity and convergence anomalies in the upper-level during Phase 1. The northeasterlies associated with the cyclonic circulation anomaly over the SCS and Philippine Sea, accompanied by the low-level divergence and negative vorticity, are not favorable for the formation of rainfall in the YRB. During Phases 2 and 3, the negative rainfall anomalies significantly weaken in the YRB and south of Japan. Also, the northeasterlies above these regions become weaker due to the weakening and shifting of northeastward cyclonic circulation with the center toward the WNP (Fig. 5, Phase_2 and 3). Phase 3 is the transition phase, during which the YRB goes through dry to wet anomalies. Note that an anomalous anticyclonic circulation starts to form in the tropical Philippine Sea in Phase 3.

About 5 days later, the organized positive rainfall anomalies in Phase 4 appear near the mid-lower reaches of the YRB. The anomalous cyclone weakens westward and the anomalous northeasterly dominates the northern part of the Yangtze River. Simultaneously, the anticyclonic anomaly over the Philippine Sea begins to strengthen and moves northward. The southern part of China is characterized by the low-level westerly anomalies, which provide the favorable circulation condition for strong precipitation in the YRB. During peak wet Phase 5, the anticyclonic anomaly continues to strengthen and propagate northward, and the northern cyclonic anomaly continues to weaken and shift westward into the adjacent region between south of Korean Peninsula and southern Japan. The enhanced rainfall along the middle and lower reaches of the Yangtze River in eastern China extends slightly northeastward under the influence of the strengthened southwesterlies to the south of the rainband and the weakened northeasterlies to the north of the rainband (Fig. 5, Phase_5). In the vertical phase evolution, the positive vorticity in the lower troposphere, the low-level convergence and upper-level divergence during Phases 4 and 5 all support the enhancement of rainfall in the YRB (Fig. 6). From Phase 6 to Phase 8, the positive rainfall anomalies begin to weaken gradually in the YRB; the associated lowlevel cyclonic anomaly disappears, and the anticyclonic anomaly weakens northward.

4.2 Composite in dry summers

For the dry-summer composite, the ISO rainfall anomalies evolve in similar ways phase-by-phase compared to
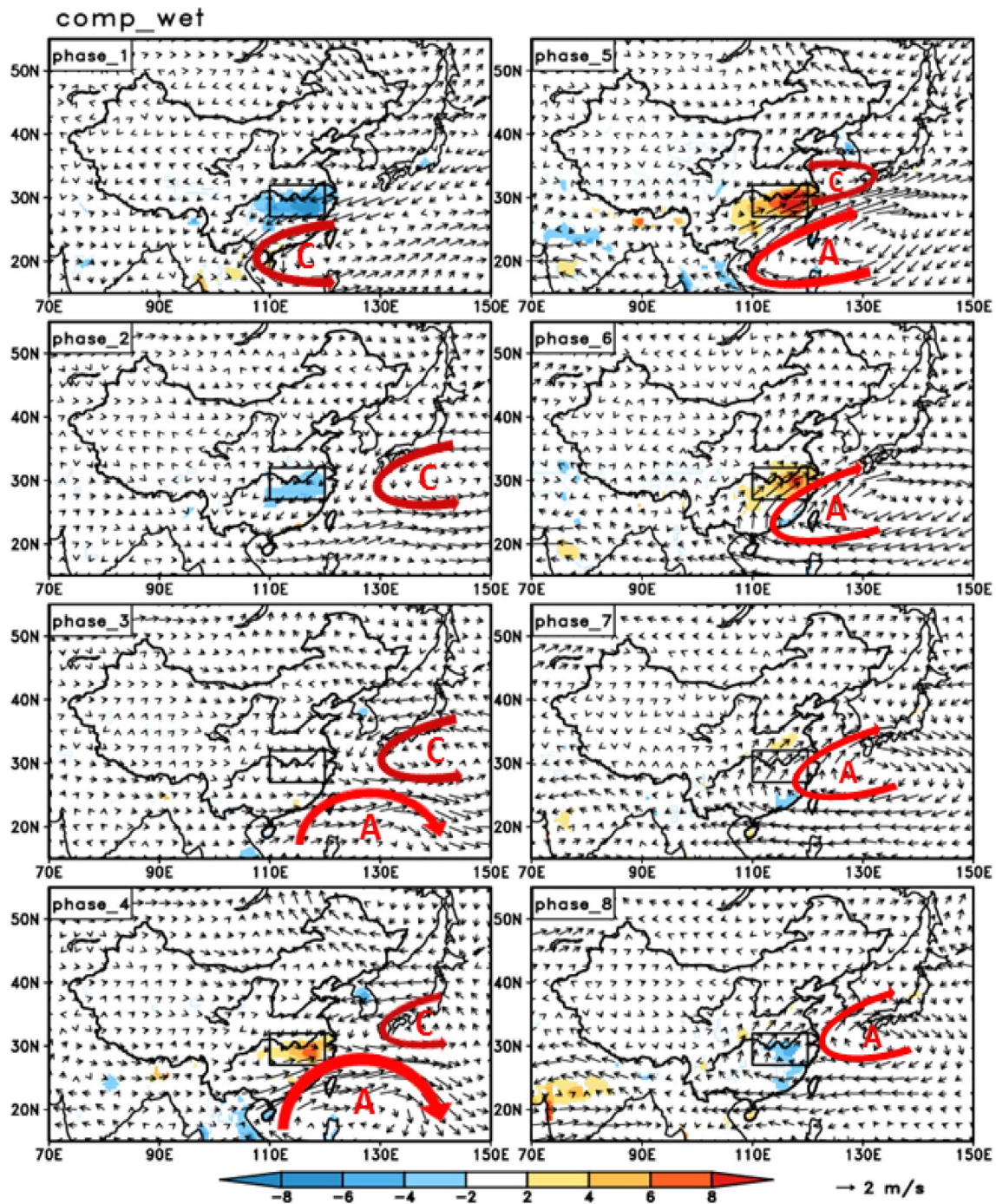
Fig. 5 Composite ISO cycle of 30–90 days filtered anomalous rainfall rate (shading in unit of mm/day) and 850-hPa wind (vectors in unit of m/s) during the wet summers. Only the rainfall anomalies that are significant above the 90% confidence level are shown. The thick red lines denote the anomalous circulations (marked with "C") and anti-circulations (marked with "A")

the composite in the wet summers, but with weaker precipitation (Fig. 7). It indicates that the YRB receives more intraseasonal precipitation during wet summers than during dry summers. This is consistent with the in-phase interannual relationship between ISO intensity and summer-mean rainfall in the YRB shown in Fig. 4. It is noted that the ISO

low-level circulation anomalies in the dry summers are quite different from those in the wet summers. Unlike the northward movement of the cyclone-anticyclone circulation pair in the wet summers, the cyclonic anomaly located in the northern Philippines decreases westward significantly from Phase 1 to Phase 3 in the dry summers (Fig. 7, Phase_1, 2,

Fig. 6 Height-phase cross section of 30–90 days filtered wind divergence/convergence (contour; unit: $\times 10^{-6}$/s) and vorticity (shading; unit: $\times 10^{-6}$/s) anomalies over the YRB in the wet summers
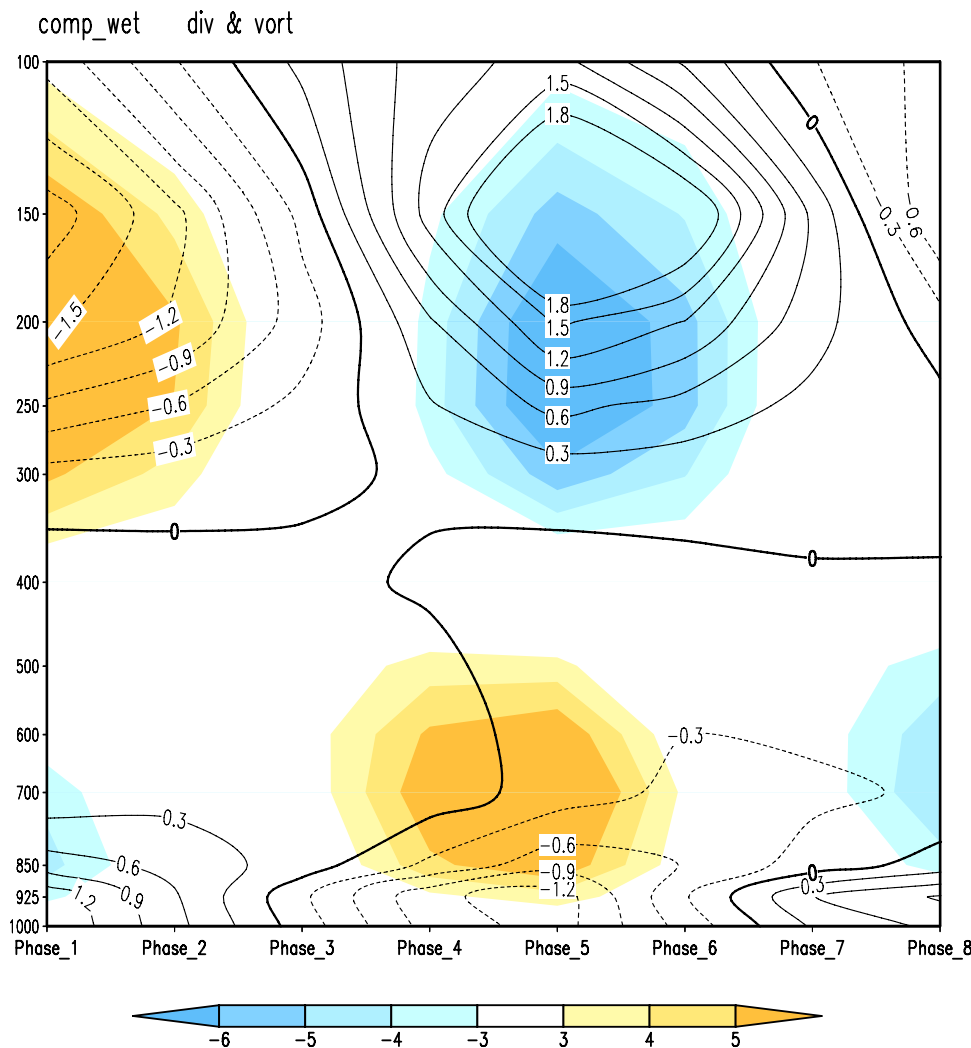
and 3). Meanwhile, an anticyclonic anomaly forms over the sea region to the southeast of Japan during Phase 2. With the intensification and westward movement of the anticyclonic circulation to southeastern China, the anomalous cyclone vanishes during the peak Phase 4 and 5 (Fig. 7, Phase_4 and 5). The precipitation in the YRB is considerably weak due to the weak of low-level wind convergence, though the strong southwesterlies dominate the regions from south to YRB of China in Phase 5. From the vertical structure, the positive vorticity in the lower troposphere, low-level convergence and upper-level divergence during the peak phase are weaker in the dry summers than that in the wet summers (Fig. 8), resulting in less precipitation in the YRB.

In brief, the northward propagation of the cyclone-anticyclone anomalous pair over East Asia from the tropics plays a critical role in producing strong precipitation in the YRB during the wet summers. In contrast, in the dry summers, the westward movement of the anomalous anticyclonic circulation and the vertical conditions do not favor strong precipitation in eastern China.

5 Water vapor flux budget diagnosis

The precipitable water in an air column is given by

$$P_\mathrm{r} = -\frac{1}{g} \int_{p_\mathrm{t}}^{p_\mathrm{b}} \left(\frac{\partial q}{\partial t} + \nabla \cdot \mathrm{V}q + \frac{\partial}{\partial p}\omega q \right) \mathrm{d}p, \tag{1}$$

where P_r is the precipitation in an air column, g is the gravity, q is the specific humidity, t is the time, V is the horizontal wind vector, ∇ is the horizontal gradient operator, p is the pressure, p_b and p_t are the bottom pressure (usually 1000 hPa) and the top pressure (300 hPa), respectively, ω is the vertical pressure velocity.

For the seasonal mean and intraseasonal variability of rainfall, and for the column integration of rainfall where $\omega = 0$ at p_b and p_t, the precipitation equation can be approximately written by the column integrated water vapor:
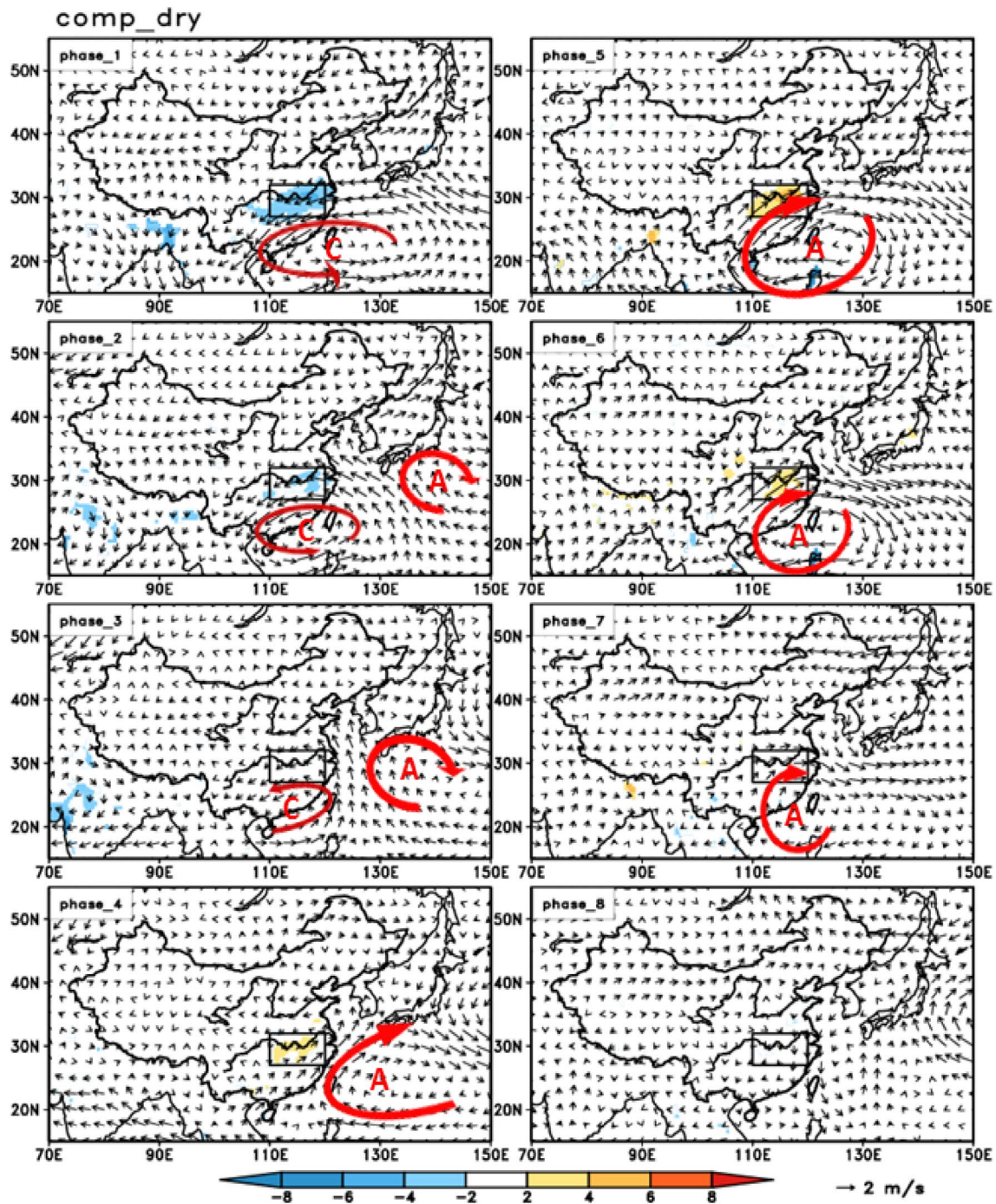
Fig. 7 Same as Fig. 5, except for the dry summers

$$P_r \approx -\frac{1}{g} \int_{p_t}^{p_b} (\nabla \cdot Vq) dp. \tag{2}$$

The above Eq. (2) indicates that the precipitation is mainly determined by the column-integrated convergence of water vapor flux, where the convergence of water vapor flux may be decomposed into two terms:

$$-\nabla \cdot Vq = -V \cdot \nabla q - q\nabla \cdot V. \tag{3}$$

The term $\langle -V \cdot \nabla q \rangle$ represents the horizontal advection of moisture; the term $\langle -q\nabla \cdot V \rangle$ represents the horizontal moisture convergence. That means the precipitation is primarily

Fig. 8 Same as Fig. 6, except for the dry summers
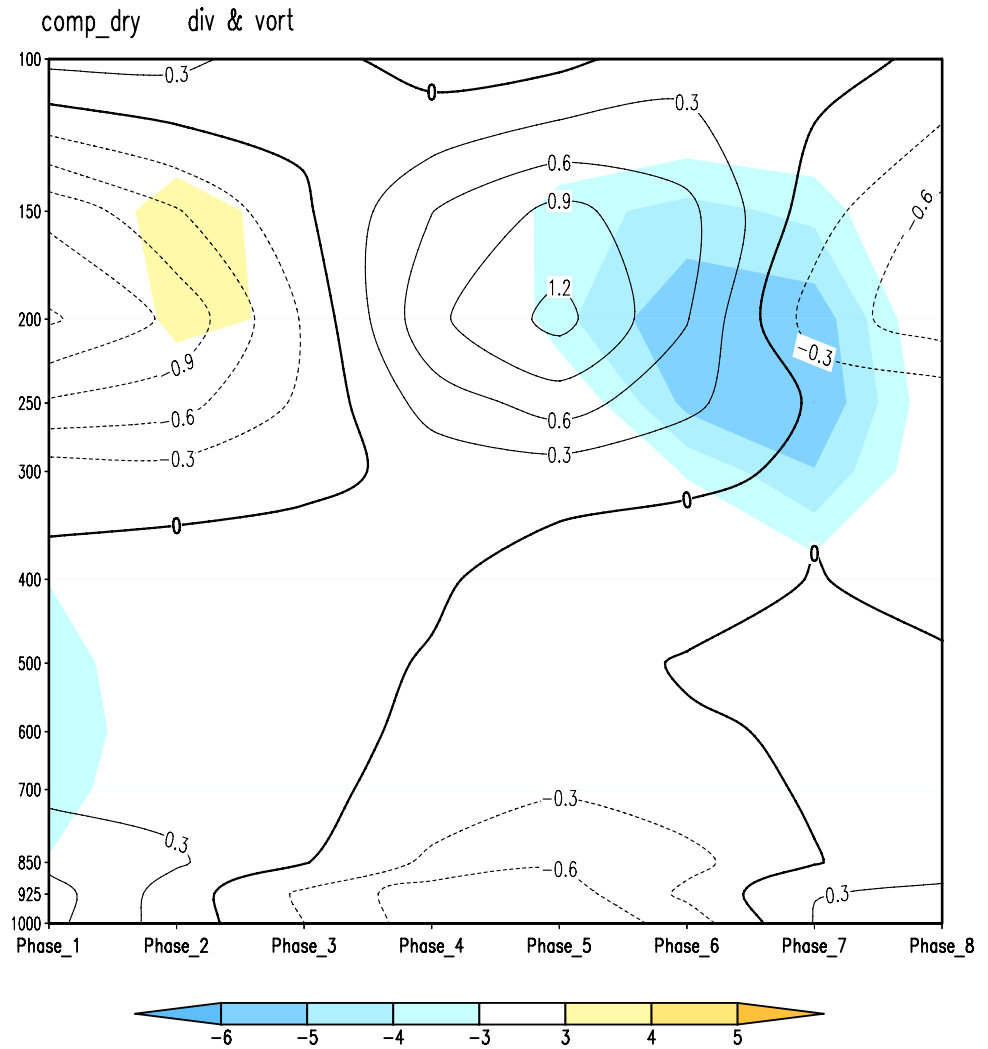
contributed by the horizontal advection of moisture and moisture convergence.

In order to illustrate the impact of multi-scale motions on the intraseasonal variation of YRB rainfall which we focused on, each variable of Eq. (3) is decomposed into a low-frequency background state (LFBS, > 90 day) component (which include climatology annual and semi-annual cycles and interannual variability), a 30–90 days intraseasonal (ISO) component, and a higher-frequency variability (HFV, < 30 day) component. For example, horizontal wind vector is decomposed into:
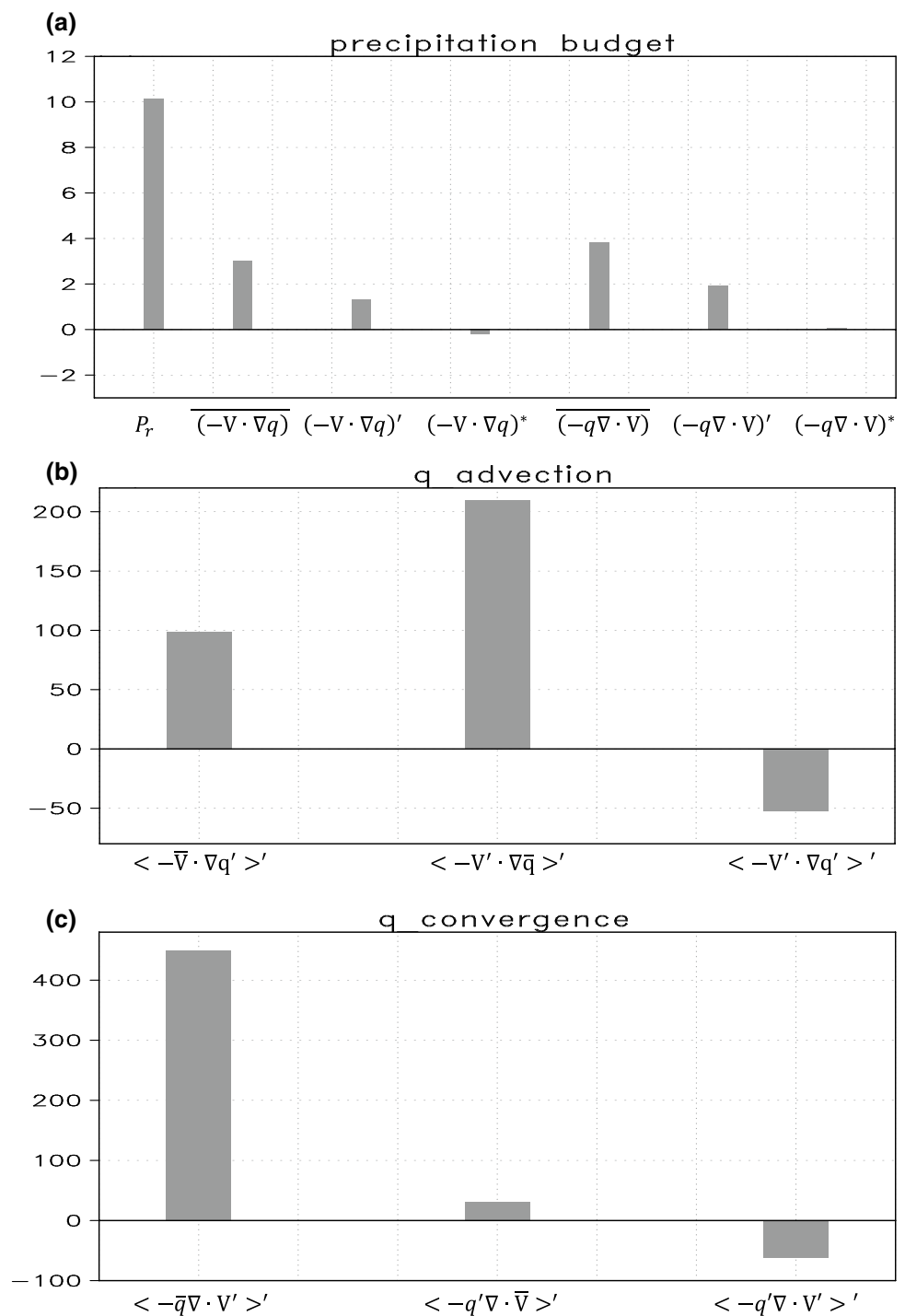
$$V = \overline{V} + V' + V^*,$$

where an overbar, a prime, and a star denote the LFBS, ISO, and HFV component, respectively. The total precipitation is the sum of the decomposed multi-timescale components of vertically integrated moisture advection and convergence terms described in Eq. (3). Our calculations of precipitation and each term of decomposed moisture advection and convergence components show in Fig. 9a that the total

precipitation is primarily attributed to LFBS and ISO components of moisture advection [i.e., $\overline{(-V \cdot \nabla q)}$, $(-V \cdot \nabla q)'$] and moisture convergence [i.e., $\overline{(-qV \cdot V)}$, $(-qV \cdot \nabla)'$]. In general, the convergence of moisture shows a much greater contribution than the advection of moisture to the precipitation. It is noted that the amplitude of HFV in both advection and convergence of moisture [$(-V \cdot \nabla q)^*$, $(-q\nabla \cdot V)^*$] is in general too small to consider its contribution to the total precipitation. For intraseasonal rainfall variability over the YRB, we note that the terms associated with the HFV interactions with the LFBS and ISO components [i.e., terms such as $\langle -\overline{V} \cdot \nabla q^* \rangle'$, $\langle -V' \cdot \nabla q^* \rangle'$, $\langle -V^* \cdot \nabla \overline{q} \rangle'$, $\langle -V^* \cdot \nabla q' \rangle'$, $\langle -V^* \cdot \nabla q^* \rangle'$ and terms such as $\langle -\overline{q}\nabla \cdot V^* \rangle'$, $\langle -q'\nabla \cdot V^* \rangle'$, $\langle -q^*\nabla \cdot \overline{V} \rangle'$, $\langle -q^*\nabla \cdot V' \rangle'$, $\langle -q^*\nabla \cdot V^* \rangle'$] are in general small in contributing to the intraseasonal moisture advection and convergence terms and thus to the first order of approximation they are negligible. Thus, the intraseasonal horizontal moisture advection and convergence terms can be written as:

$$\langle -V \cdot \nabla q \rangle' \approx \langle -\overline{V} \cdot \nabla q' \rangle' + \langle -V' \cdot \nabla \overline{q} \rangle' + \langle -V' \cdot \nabla q' \rangle', \quad (4)$$

Fig. 9 **a** Precipitation budget with column integrated (1000–300 hPa) LFBS, ISO and HFV moisture advection and convergence terms over region of (110°–120°E, 27°–32°N). From left to right, observed precipitation, following three terms of moisture advection in LFBS, ISO and HFV components, the last three terms of LFBS, ISO and HFV moisture convergence components are shown (unit: mm/day). **b** Difference of intraseasonal moisture advection individual component terms by calculating integrated intraseasonal water vapor flux budget at peak Phase 5 between wet and dry summers (wet minus dry) over the YRB. **c** As in **b**, but for the intraseasonal moisture convergence terms [unit: 10^{-8} kg/(m^2 s)]

$$\langle -q\nabla \cdot V \rangle' \approx \langle -\overline{q}\nabla \cdot V' \rangle' + \langle -q'\nabla \cdot \overline{V} \rangle' + \langle -q'\nabla \cdot V' \rangle'. \quad (5)$$

To identify the relative contributions to the anomalous precipitation along the YRB region, the impact of LFBS, ISO and HFV components are computed quantitatively according to Eqs. (4) and (5). Applying a 90-day low-pass filter, 30-90-day band-pass filter and a 30-day high-pass filter to each variable of above equations, one may extract the LFBS, ISO and HFV signals from the original data, respectively.

To reveal the impact of the interannual and intraseasonal variation mode on the ISO rainfall in the YRB, a vertical integrated (1000–300 hPa) moisture advection and convergence analysis with different decomposed timescale is calculated quantitatively over the YRB region of

(110°–120°E, 27°–32°N). Figure 9b shows the contributions of moisture advection from each term of Eq. (4) in the wet and dry summers. The largest positive contribution to the ISO rainfall is the term of $\langle -V' \cdot \nabla \overline{q} \rangle'$, which is associated with the advection of mean moisture by the ISO flow. The second large positive term is the advection of ISO anomalous moisture by the mean flow $\langle -\overline{V} \cdot \nabla q' \rangle'$. Its magnitude is two times smaller than the mean moisture advected by the ISO flow. The third term $\langle -V' \cdot \nabla q' \rangle'$, which denotes the ISO moisture advected by the ISO flow, induces a negative ISO rainfall tendency. These positive contributions of $\langle -V' \cdot \nabla \overline{q} \rangle'$ and $\langle -\overline{V} \cdot \nabla q' \rangle'$ to the ISO rainfall demonstrate that the mean moisture advected by the ISO anomalous flow and the anomalous moisture advected by the mean flow play an important role in the occurrence and maintenance of intraseasonal anomalous rainfall in the YRB during summer. However, the ISO–ISO interactions $\langle -V' \cdot \nabla q' \rangle'$ on the intraseasonal-timescale tend to produce negative contribution to the ISO rainfall. The intraseasonal moisture advection by the intraseasonal flow is more favorable for the dry summers.

In addition to the moisture advection, the effect of moisture convergence on the intraseasonal rainfall is also examined. Figure 9c illustrates the moisture convergence contributions to the ISO rainfall variability from each term of Eq. (5). The two terms of $\langle -\overline{q} \nabla \cdot V' \rangle'$ and $\langle -q' \nabla \cdot \overline{V} \rangle'$ show the positive contribution to produce the intraseasonal rainfall. The leading term $\langle -\overline{q} \nabla \cdot V' \rangle'$, which represents the convergence of mean moisture by the ISO flow, is dominant in these three components. It indicates that the abundant summer mean moisture is the critical factor in causing the strong ISO rainfall. The second term $\langle -q' \nabla \cdot V \rangle'$, associated with the mean flow convergence by the ISO moisture, also plays a positive role in the maintenance of ISO rainfall, although it only accounts for about 8% of the total ISO moisture convergence contribution. This result is consistent with Hus and Li (2012), who emphasized that much greater contribution of $\langle -q \nabla \cdot V \rangle'$ than $\langle -q' \nabla \cdot V \rangle'$. That is because of the large difference between the mean and intraseasonal moisture amplitude in the precipitation region. The term $\langle -q' \nabla \cdot V' \rangle'$, intraseasonal eddy–eddy moisture convergence, same as the interactions of moisture advection, exhibits a negative role in the contribution to the ISO rainfall.

It is noted that the magnitude of mean moisture convergence by ISO flow is about 2–4 times larger than the moisture advection terms (Fig. 9b, c). It is suggesting that the convergence of mean moisture dominates the moisture advection for the maintenance of anomalous rainfall over the YRB during wet summers. This result is consistence with Ding and Hu (2003), who demonstrated that the strong precipitation came mainly from the convergence of water vapor in the low-level troposphere. In this study, the diagnostic analysis further shows that the processes of increased mean moisture convergence by ISO flow and mean moisture advection by ISO flow are crucial for supporting and producing the anomalous rainfall in YRB region.

According to the previous studies (Chen 1985; Huang and Sun 1992, 1998; Ding and Hu 2003), the water vapor transport and convergence of water vapor flux play an important role in contributing to summer rainfall in the East Asian monsoon region. The relationship between the atmospheric large-scale circulation and water vapor transport can be illustrated by means of the streamfunction and water vapor flux potential fields. During boreal summer, there are strong westward moisture transport from the tropical Pacific and strong eastward moisture transport from tropical Indian Ocean (Fig. 10a). The abundant moist air is transported from the tropical oceans toward eastern China to support the local precipitation. During the wet summer, anomalous southwesterlies associated with the anticyclonic circulation over the SCS and WNP increase the moisture in the YRB region (Fig. 11a). In addition to water vapor transport, the convergence of water vapor flux represented by the potential and divergence fields plays an essential role in maintaining the high mean and anomalous water vapor content in the YRB (Figs. 10b, 11a). In the dry summers, on the contrary, anomalous moisture divergence and a negative moisture anomaly appear in the region (Fig. 11b). It is likely that the interannual variation of the East Asian summer monsoon is modulated by the Pacific-Japan (PJ) pattern (Nitta 1987; Huang and Sun 1992). Such a PJ pattern may be inferred from Fig. 11, which shows an alternated dry-wet-dry pattern. In addition, the interannual variability of ISO also shows a close relationship with the PJ pattern. Figure 12 indicates that the ISO precipitation over the YRB is strongly influenced by the teleconnection pattern of intraseasonal water vapor flux transport anomalies, which is denoted by the various cells with negative and positive centers over East Asia. It suggests that the PJ pattern of water vapor flux not only modulates the interannual variation of East Asian summer monsoon, but also has an impact on the interannual variability of ISO precipitation in the YRB. Thus, the background seasonal-mean state is important in modulating the ISO variability.

In the composites of vertical profiles averaged over the YRB during the wet and dry summers, one can see that all the variables in Fig. 13 show remarkable differences between the wet and dry summers. During the wet summers, the moisture increases upward from the boundary layer and reaches the maximum at 700 hPa (Fig. 13a) due to the strong ascending motion (Fig. 13b). Accompanied by the pronounced ascending motion, the distribution of low-level convergence and upper-level divergence in the troposphere favors the buildup of local moisture through moisture flux convergence (Fig. 13c). Same as specific humidity, the anomalies of vertical motion
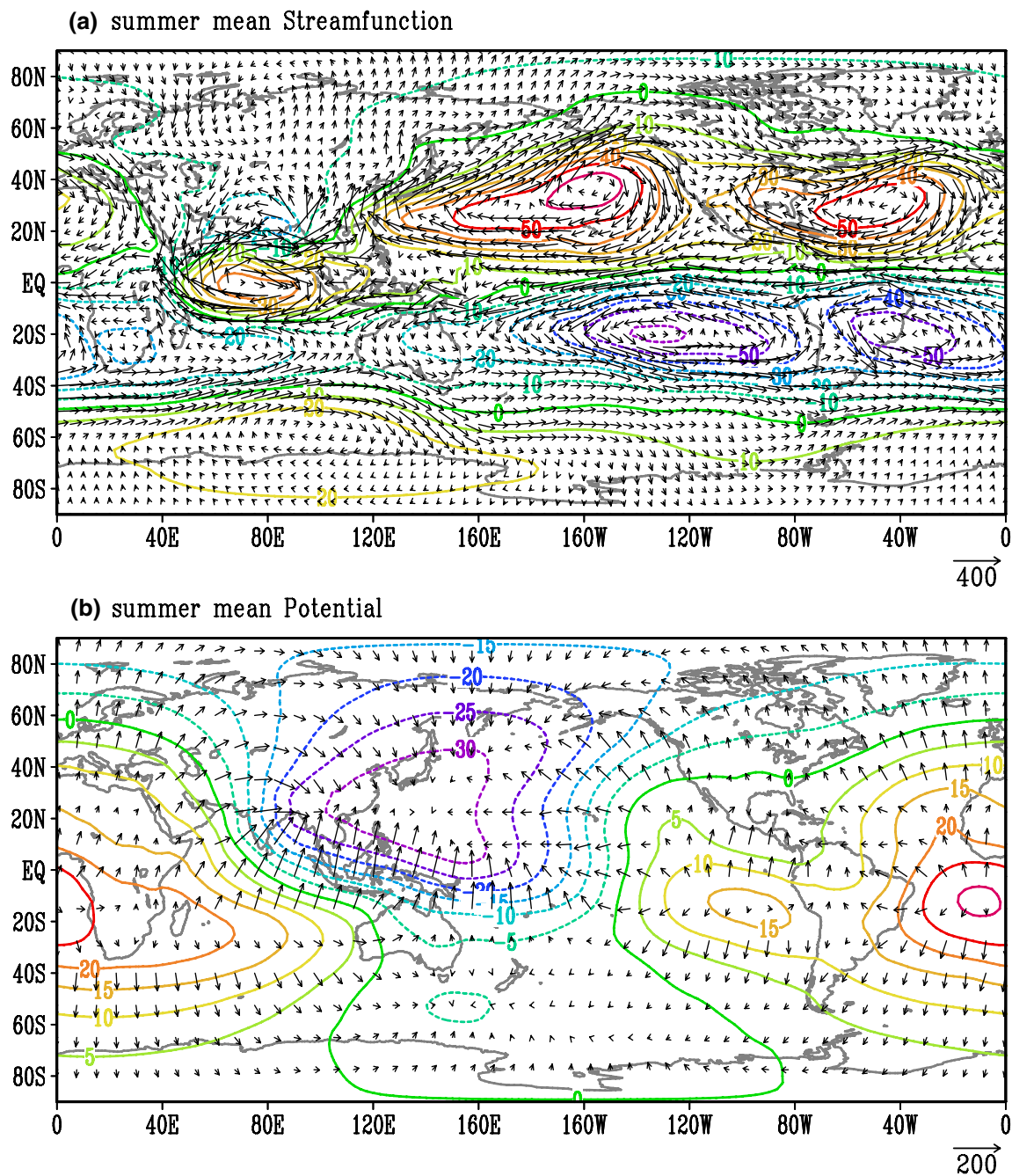
(a) summer mean Streamfunction

(b) summer mean Potential

Fig. 10 Distribution of **a** streamfunction and non-divergent field, and **b** potential and divergent field for the vertically integrated water vapor flux during summer (MJJA). Streamfunction and potential are indicated by contours, unit: 10^7 kg/s; non-divergent and divergent fields are indicated by vectors, unit: kg/(m s)

and divergence/convergence, the vertical shear of zonal wind also show opposite signs between the wet and dry summers from the boundary layer to the upper level (Fig. 13d). The negative vertical shear anomaly in the wet summers implies that the easterlies decrease rapidly from the lower to upper troposphere until the westerlies appear at 200 hPa, indicating an anomalous westerly shear appears during the wet summer. Given the summer mean westerly shear over the region, the westerly shear anomaly implies an enhanced total vertical wind shear over the Meiyu front region. The strong vertical shear may destabilize the intraseasonal perturbation and enhance the strength of ISO (Wheeler and Kiladis 1999). During the dry summers, however, less moisture, downward motion, divergence in the lower troposphere and
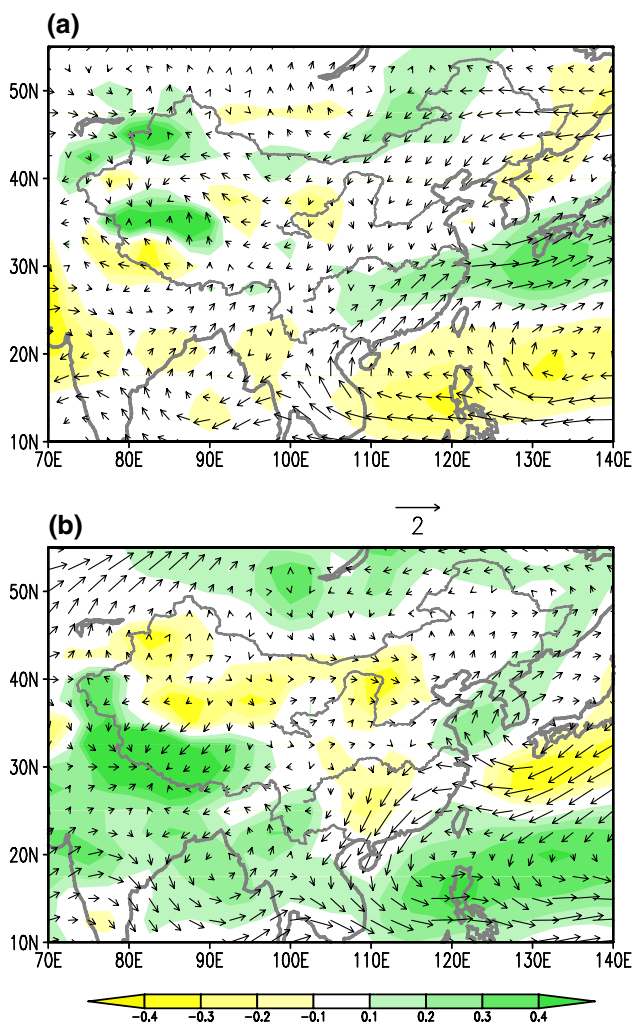
(a)

(b)

Fig. 11 Composite anomaly patterns of summer (MJJA) wind (vector; unit: m/s) and specific humidity (shading; unit: g/kg) at 850 hPa in the wet (**a**) and dry (**b**) summers

weaker vertical shear over the YRB are not favorable for the development of ISO (Fig. 13).

6 Effect of ISO perturbation on summer rainfall

Besides the ISO rainfall, the intraseasonal anomalous low-level vorticity, convergence and specific humidity over the YRB all show larger intensity in the wet summers than in the dry summers. These results confirm the high positive correlation between the summer rainfall in the YRB and ISO intensity on the interannual timescale. Based on the relationship, the feedback of ISO perturbation to the summer-mean precipitation is investigated.

Figure 14 shows height-phase sections of ISO rainfall, omega and specific humidity in the YRB during the wet

and dry summers, respectively. With the commencement of precipitation at Phase 3 (Fig. 14a), the ascending motion starts to enhance in the boundary layer in Phase 2 and then increases rapidly during peak Phase 4 and 5 in the wet summers (Fig. 14b). The peak phase is featured by positive moisture anomalies in the YRB with a deep enhanced water vapor layer in the mid-lower troposphere below 300 hPa (Fig. 14c). The enhanced specific humidity during Phase 4–5 and increased temperature during the two phases (figure not shown) lead to an increase of equivalent potential temperature and moist static energy (MSE) in the lower troposphere (Zhao et al. 2013). This marked increase of equivalent potential temperature and MSE result in a convectively unstable stratification, which favors the occurrence of a stronger ISO variability. In the dry summers, however, the ISO rainfall, vertical motion and specific humidity anomalies are all weaker in magnitude compared to those in the wet summers. The little amount of water vapor in the dry summers is not enough to produce and support the strong and persistent rainfall in the YRB (Fig. 14f). More importantly, compared to the ascending motion in the boundary layer in the wet summers, it appears the descending motion in the YRB in the boundary layer below 900 hPa from Phase 4 in the dry summers (Fig. 14e). It is therefore inferred that the vertical motion may play an essential role in modulating the rainfall in the YRB. What causes the subsidence in the boundary layer in the YRB during the dry summers? To answer this question, the omega equation is diagnosed to identify the factor(s) that determine the ascending or descending motion in the boundary layer in the YRB.

The quasi-geostrophic omega equation without diabatic heating may be written as:

$$\left(\nabla^2 + \frac{f^2}{\sigma}\frac{\partial^2}{\partial p^2}\right)\omega = \frac{f}{\sigma}\frac{\partial}{\partial p}[V \cdot \nabla(f + \zeta)] + \frac{R}{\sigma p}\nabla^2(V \cdot \nabla T),$$

(6)

where σ denotes the static stability, ∇ is the horizontal gradient operator, ∇^2 is the Laplacian operator, f is the Coriolis parameter, p is pressure, ω is vertical p velocity, R is the gas constant, V represents horizontal velocity vector, and ζ is relative vorticity.

From Eq. (6), we can conclude that the vertical motion is primarily determined by two terms. One is the vorticity advection associated with vertical motion; the other is the horizontal variation of temperature advection. If we assume

$$A_\zeta = -V \cdot \nabla(f + \zeta),$$

and $A_T = -V \cdot \nabla T$, then the terms on the right hand side of Eq. (6) can be simplified as:

$$\left(\nabla^2 + \frac{f^2}{\sigma}\frac{\partial^2}{\partial p^2}\right)\omega = -\frac{f}{\sigma}\frac{\partial A_\zeta}{\partial p} - \frac{R}{\sigma p}\nabla^2 A_T.$$

(7)

Fig. 12 Composite distribution of 30–90 days filtered streamfunction (contour; unit: 10^7 kg/s) and non-divergent field [vector; unit: kg/(m s)] for the vertically integrated water vapor flux at peak phase of ISO precipitation during wet summers
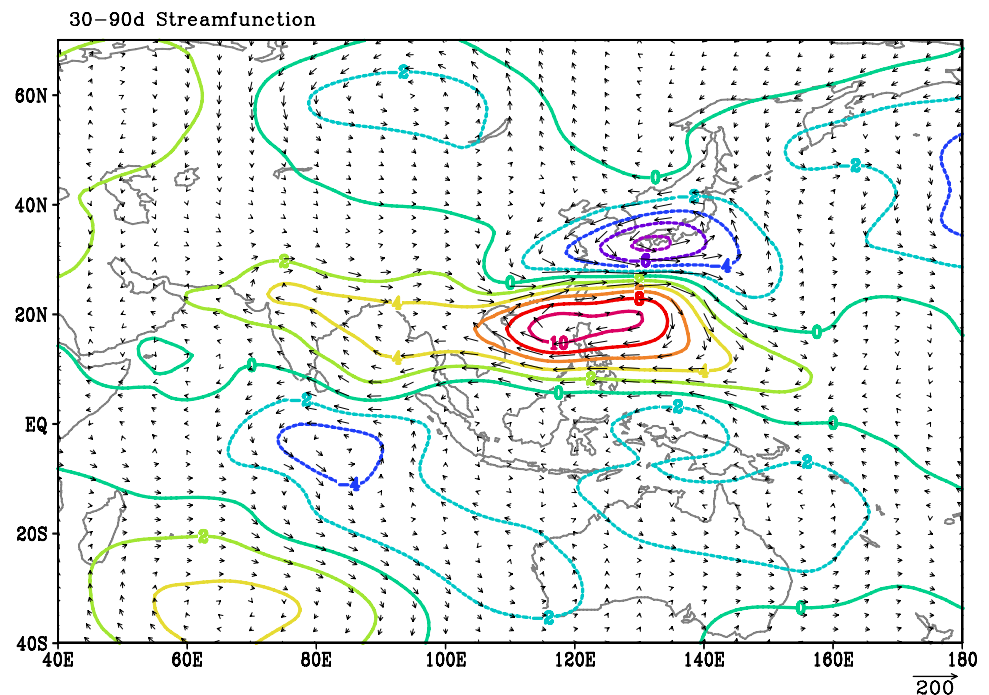
The vertical motion depends on the contributions of vertical differentiation of vorticity advection A_ζ and horizontal distribution of temperature advection A_T. The warm advection and positive vorticity advection increases with height can cause ascending motion, whereas the cold advection and positive vorticity advection decreases with height will result in descending motion. To reveal the significant contributor that causes the upward or downward motion in the YRB, the terms of temperature advection and vertical differentiation of horizontal vorticity advection on the right hand side of Eq. (7) are diagnosed during the wet and dry summers.

The height-phase cross section of 30–90 days filtered anomalous temperature advection (A_T) in the YRB in the wet and dry summers are shown in Fig. 15. A_T is positive in the mid- and lower-troposphere during the peak phase in both wet and dry summers. It means that the warm advection contributes to the ascending motion in the YRB in both wet and dry summers. Note that the transition between the cold advection and warm advection happens in Phase 3. The warm advection increases rapidly in Phase 4 and shows larger anomalies during the wet summers than during the dry summers (Fig. 15).

In the composite of vertical differentiation of vorticity advection, the positive vorticity advection (A_ζ) anomalies increase with height in the boundary layer and peak at Phase 3 in the wet summers (Fig. 16a). Phase 5 is the transition from positive to negative vorticity advection in the lower troposphere. The increase with height of positive vorticity advection during Phases 3 and 4 causes upward motion, although it is weak. In the dry summers, by contrast, the

A_ζ decreases with height from Phase 3 and peaks during Phases 5 and 6 (Fig. 16b) in the boundary layer. The increase (decrease) with height of A_ζ in the boundary layer during peak phase in the wet (dry) summers explains why there is ascending (descending) motion in the wet (dry) summers in the boundary layer (Fig. 15b, e).

During the wet summers, the increase of positive A_ζ anomalies with height, together with warm advection, contributes to the ascending motion in the boundary layer, which brings about more precipitation in the YRB. On the contrary, the decrease of A_ζ with height results in subsidence in the boundary layer in the dry summers. Though the warm advection causes upward motion in the dry summers, the ascending motion is less strong than the descending motion resulted from A_ζ. The descending motion in the boundary layer in the YRB impedes the convergence of moisture which is the necessary condition for precipitation. Thus, the vertical motion that impacts significantly on the precipitation in the YRB is primarily attributed to the vertical differentiation of A_ζ.

7 Summary and discussion

The summer rainfall in eastern China exhibits remarkable intraseasonal and interannual variations. The spectral analysis of summer rainfall shows that the 30–90 days is the dominant mode in the intraseasonal variability of climatological summer rainfall in the YRB. The interannual variation of summer rainfall in the YRB displays a significant positive
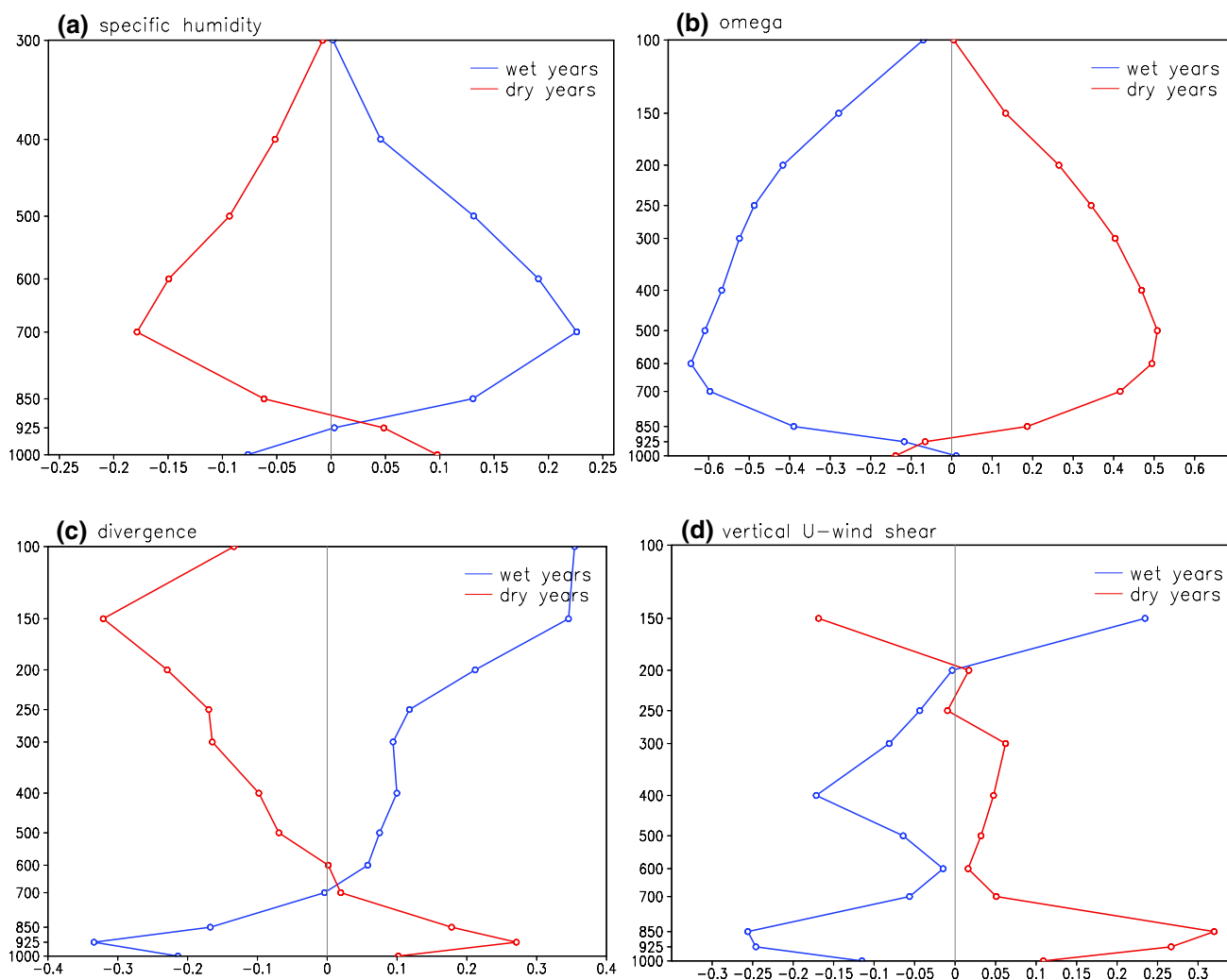
Fig. 13 Composite vertical profiles of **a** specific humidity (unit: g/kg), **b** vertical pressure velocity (unit: 10^{-2} Pa/s), **c** wind divergence (unit: 10^{-6}/s), and **d** vertical zonal wind shear (unit: m/s) averaged over the YRB during MJJA. The blue (red) curve denotes the composite for the wet (dry) summers

correlation with the 30–90 days summertime ISO intensity in situ. It is suggested that a rainy (dry) season is usually associated with strengthened (weakened) ISO activity in summer over the YRB in eastern China.

The spatial structure and temporal evolution of composite ISO associated with the summer rainfall and 850-hPa wind in East Asia are analyzed for both wet and dry summers in the YRB. The comparison of ISO structural and evolutionary characteristics between the wet and dry summers shows that their low-level circulation anomalies are quite different. In the wet summers, the cyclone-anticyclone circulation pair propagates northward from the tropics over East Asia. In contrast, the low-level cyclonic anomaly in the dry summers weakens dramatically as it moves westward. Accompanied by the westward propagation of developing anticyclonic anomaly, the cyclonic anomaly disappears in situ during the dry summers. The wind convergence, upward motion and

abundant moisture in the lower troposphere in the wet summers provide favorable conditions for strong precipitation in the YRB. However, the wind convergence and moisture are considerably weaker during the dry summers.

The budget diagnosis of water vapor flux shows that the moisture advection provides positive support for maintenance of intraseasonal rainfall in the YRB. The mean moisture convergence by the ISO flow plays an important role in contributing to the ISO rainfall in the YRB. In the decomposed terms of moisture advection and moisture convergence, the maximum contributions to the ISO rainfall primarily comes from the seasonal mean moisture because of its much greater amplitude (Hus and Li 2012). The moist air originated from the tropics is transported northward to the YRB by the mean flow of the southwesterlies, which is associated with the strong anticyclonic circulation over the SCS and WNP. Also the variables of wind convergence,
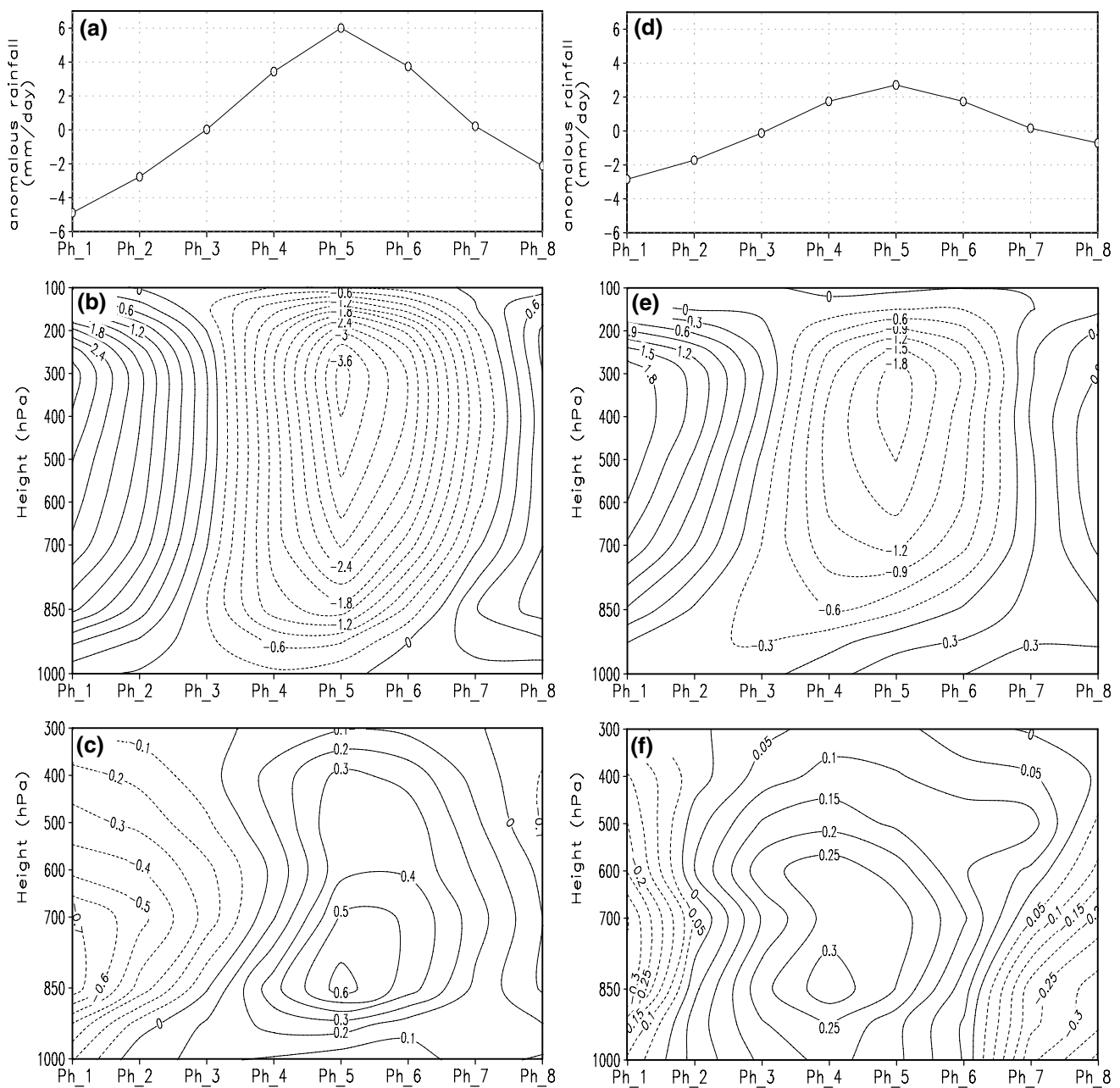
Fig. 14 Height-phase cross section of 30–90 days filtered precipitation rate (**a**; unit: mm/day), pressure vertical velocity (**b**; unit: 10^{-2} Pa/s) and specific humidity (**c**; unit: g/kg) over the YRB during the wet summers. **d–f** The 30–90 days filtered precipitation rate, pressure vertical velocity and specific humidity during the dry summers, respectively

vertical motion, buildup of low-level moisture, and vertical wind shear contribute to the development of ISO over the YRB in eastern China. From these large scale background conditions, it indicates that the mean state plays an essential role in controlling of ISO perturbation.

The feedback of ISO perturbation to the summer mean precipitation is investigated in terms of the structural and evolutional characteristics of ISO. It is found that the intraseasonal vertical motion is upward (downward) in the

boundary layer in the peak phase in the YRB during the wet (dry) summers. The diagnosis of anomalous vertical motion equation shows that temperature advection has the same contribution in both wet and dry summers. The ascending (descending) motions in the boundary layer during the wet (dry) summers are primarily attributed to the vertical differentiation of horizontal vorticity advection. In the dry summers, the effect of temperature advection is weaker than the effect of the vertically differentiated vorticity advection.
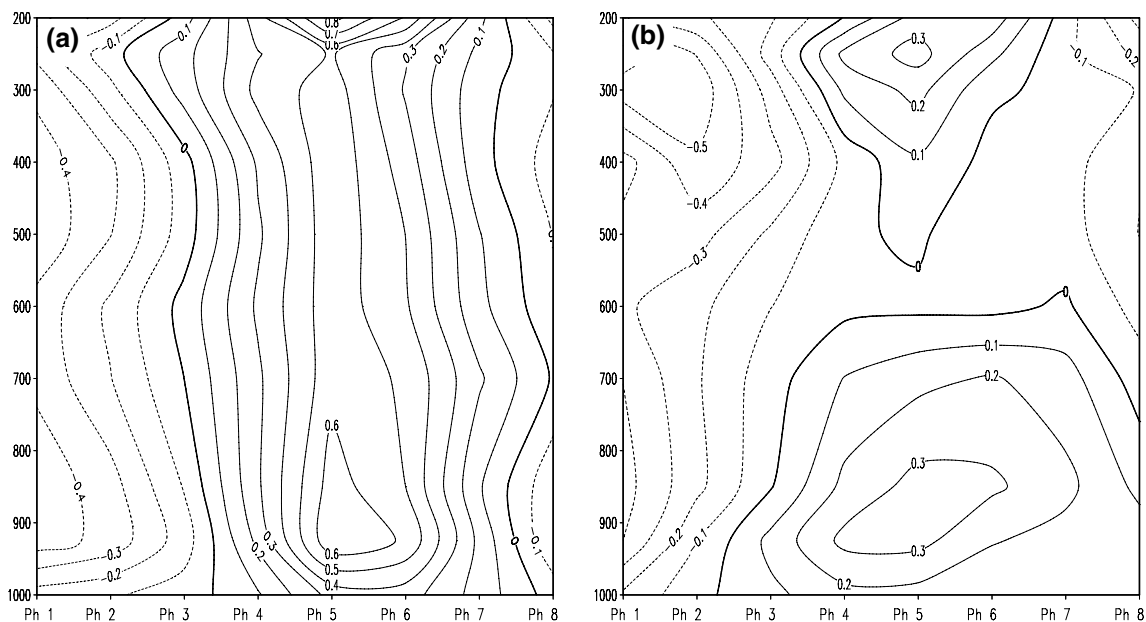
Fig. 15 Vertical profile of the 30–90 days filtered temperature advection over the YRB during the wet (**a**) and dry (**b**) summers. Unit: 10^{-5} °C/s
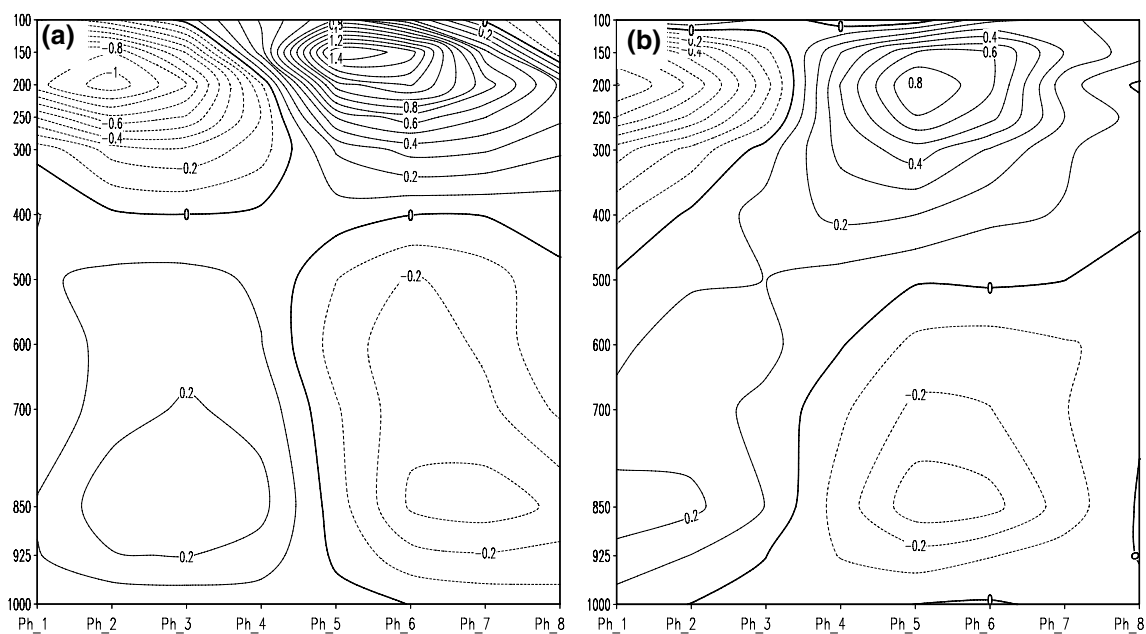

Fig. 16 Vertical profile of the vertical differentiation of 30–90 days filtered vorticity advection over the YRB during the wet (**a**) and dry (**b**) summers. Unit: $\times 10^{-10}/s^2$

Thus, the latter is the major impact factor on the vertical motion in the boundary layer. The strong upward motion in the lower troposphere during the wet summers provides crucial condition for the strong precipitation in the YRB. The high positive correlation between the intensity of summertime ISO and the summer-mean precipitation over the YRB suggests a possible two-way interaction scenario. On the one hand, a stronger mean vertical motion and moisture condition favors a stronger ISO activity. On the other hand, a greater ISO may enhance the summer-mean precipitation as rainfall is positive-only event. Multiple heavy rainfall events help elevate total precipitation.

While the current study reveals a close relation between the ISO and mean precipitation, some issues remain open and need to be further addressed. It has been shown that the ISO intensity, movement or frequency is greatly modulated

by the annual cycle of the mean state (e.g., Madden 1986; Wang and Rui 1990; Hartmann et al. 1992; Li and Wang 2005; Qi et al. 2008). How do the different mean states (e.g., a wet vs. a dry summer) impact the ISO structure and propagation over the East Asia sector? What is the impact of mid-high latitude perturbations on intraseasonal rainfall variability over the YRB? What is the nonlinear rectification of the ISO on the mean state? These questions need to be further studied in future.

References

Annamalai H, Slingo JM (2001) Active/break cycles: diagnosis of the intraseasonal variability of the Asian summer monsoon. Clim Dyn 18:85–102

Chen TC (1985) Global water vapor flux and maintenance during FGGE. Mon Weather Rev 113:1801–1819

Chen Y, Zhai P (2017) Simultaneous modulations of precipitation and temperature extremes in Southern parts of China by the boreal summer intraseasonal oscillation. Clim Dyn. https://doi.org/10.1007/s00382-016-3518-4

Chen TC, Yen MC, Weng SP (2000) Interaction between the summer monsoon in East Asia and the South China Sea: intraseasonal monsoon modes. J Atmos Sci 57:1373–1392

Chen L, Zhu C, Wang W, Zhang P (2001) Analysis of 30–60-day low-frequency oscillation over Asia during 1998 SCSMEX. Adv Atmos Sci 18:623–638

Diao Y-F, Li T, Hsu P-C (2018) Influence of the boreal summer intraseasonal oscillation on extreme temperature events in the northern hemisphere. J Meteorol Res 32(4):534–547. https://doi.org/10.1007/s13351-018-8031-8

Ding Y, Hu G (2003) A study on water vapor budget over China during the 1998 severe flood periods. Acta Meteorol Sin 61(2):129–145 **(in Chinese)**

Ding Y, Wang Z (2008) A study of rainy season in China. Meteorol Atmos Phys 100:121–138

Gao M, Yang J, Wang B, Zhou S, Gong D, Kim S (2017) How are heat waves over Yangtze River valley associated with atmospheric quasi-biweekly oscillation? Clim Dyn. https://doi.org/10.1007/s00382-017-3526-z

Hartmann DL, Michelsen ML, Klein SA (1992) Seasonal variations of tropical intraseasonal oscillations: a 20–25-day oscillation in the western Pacific. J Atmos Sci 49:1277–1289

Hsu HH, Weng CH (2001) Northwestward propagation of the intraseasonal oscillation in the western North Pacific during the Boreal summer: structure and mechanism. J Clim 14:3834–3850

Huang R, Sun F (1992) Impact of the tropical western Pacific on the East Asian summer monsoon. J Meteorol Soc Jpn 70:243–256

Huang R, Zhang Z, Huang G, Ren B (1998) Characteristics of the water vapor transport in East Asian monsoon region and its difference from that in south Asian monsoon region in summer. Chin J Atmos Sci 22:460–469 **(in Chinese)**

Hus P-C, Li T (2012) Role of the boundary layer moisture asymmetry in causing the eastward propagation of the Madden—Julian oscillation. J Clim 25:4914–4931

Hus P-C, Li T, You L, Gao J, Ren H (2015) A spatial-temporal projection model for 10–30 day rainfall forecast in South China. Clim Dyn 44:1227–1244

Hus P-C, Lee J-Y, Ha K-J (2016) Influence of boreal summer intraseasonal oscillation on rainfall extremes in southern China. Int JClimatol 36:1403–1412. https://doi.org/10.1002/joc.4433

Jiang X, Li T, Wang B (2004) Structures and mechanisms of the northward propagating boreal summer intraseasonal oscillation. J Clim 17:1022–1039

Lau KM, Chan PH (1986) Aspects of the 40–50 day oscillation during the northern summer as inferred from outgoing longwave radiation. Mon Weather Rev 114:1354–1367

Lau KM, Yang GJ, Shen SH (1988) Seasonal and intraseasonal climatology of summer monsoon rainfall over East Asia. Mon Weather Rev 114:18–37

Lee J-Y, Wang B, Wheeler MC, Fu X, Waliser DE, Kang IS (2013) Real-time multivariate indices for the boreal summer intraseasonal oscillation over the Asian summer monsoon region. Clim Dyn 40:493–509

Li C (1992) An analytical study on the precipitation in the flood period over Huabei area. Acta Meteorol Sin 50:41–49 **(in Chinese)**

Li T (2010) Monsoon climate variabilities. In: Sun DZ, Frank B (eds) Climate dynamics: Why does climate vary? Geophysical Monograph Series. American Geophysical Union, Washington DC. https://doi.org/10.1029/2008GM000782

Li T (2014) Recent advance in understanding the dynamics of the Madden–Julian oscillation. J Meteorol Res 28:1–33

Li G, Li C (1999) Drought and flood in the Changjiang–Huaihe River basin associated with the multi-time-scale oscillation. Chin J Atmos Sci 23:39–50 **(in Chinese)**

Li T, Wang B (2005) A review on the western North Pacific monsoon: synopotic-to-interannual variabilities. Terr Atmos Ocean Sci 16:285–314

Li C, Li T, Lin A, Gu D, Zheng B (2015) Relationship between summer rainfall anomalies and sub-seasonal oscillations in South China. Clim Dyn 44:423–439

Lu E, Ding Y (1996) Low frequency oscillation in east Asia during the 1991 excessively heavy rain over Chingjiang–Huai River basin. Acta Meteorol Sinica 54:730–736 **(in Chinese)**

Madden RA (1986) Seasonal variations of the 40–50-day oscillation in the tropics. J Atmos Sci 43:3138–3158

Mao J, Wu G (2006) Intraseasonal variations of the Yangtze rainfall and its related atmospheric circulation features during the 1991 summer. Clim Dyn 27:815–830

Mao J, Sun Z, Wu G (2010) 20-50-day oscillation of summer Yangtze rainfall in response to intraseasonal variations in the subtropical high over the western North Pacific and South China Sea. Clim Dyn 34:747–761

Nakazawa T (1992) Seasonal phase lock of intraseasonal variation during the Asian summer monsoon. J Meteorol Soc Jpn 70:597–611

Nitta T (1987) Convective activities in the tropical western Pacific and their impact on the Northern Hemisphere summer circulation. J Meteorol Soc Jpn 64:373–390

Oh H, Ha K-J (2015) Thermodynamic characteristics and responses to ENSO of dominant intraseasonal modes in the East Asian summer monsoon. Clim Dyn 44:1751–1766

Qi Y, Zhang R, Li T, Wen M (2008) Interactions between the summer mean monsoon and the intraseasonal oscillation in the Indian monsoon region. Geophys Res Lett 35:L17704. https://doi.org/10.1029/2008GL034517

Qi Y, Zhang R, Zhao P, Zhai P (2013) Comparison of the structure and evolution of intraseasonal oscillations before and after onset of the Asian summer monsoon. Acta Meteorol Sin 27:684–700

Qi Y, Zhang R, Li T (2016) Structure and evolution characteristics of atmospheric intraseasonal oscillation and its impact on the summer rainfall over the Yangtze River basin in 1998. Chin J Atmos Sci 40:451–462 **(in Chinese)**

Ren X, Yang XQ, Sun X (2013) Zonal oscillation of western pacific subtropical high and subseasonal SST variations during Yangtze persistent heavy rainfall events. J Clim 26:8929–8946

Shen Y, Xiong A (2015) Validation and comparison of a new gauge-based precipitation analysis over mainland China. Int J Climatol. https://doi.org/10.1002/joc.4341

Tao SY, Chen LX (1987) A review of recent research on the East Asian summer monsoon in China. In: Chang CP, Krishnamurti TN (eds) Monsoon meteorology. Oxford University Press, Oxford, pp 60–92

Wang B, Rui H (1990) Synoptic climatology of transient tropical intraseasonal convection anomalies: 1975–1985. Meteorol Atmos Phys 44:43–61

Wang B, Xu X (1997) Northern Hemisphere summer monsoon singularities and climatological intraseasonal oscillation. J Clim 10:1071–1085

Wang B, Webster P, Kikuchi K, Yasunari T, Qi Y (2006) Boreal summer quasi-monthly oscillation in the global tropics. Clim Dyn 27:661–675

Wheeler M, Kiladis GN (1999) Convectively coupled equatorial waves: analysis of clouds and temperature in the wavenumber–frequency domain. J Atmos Sci 56:374–399

Yang H, Li C (2003) The relation between atmospheric intraseasonal oscillation and summer severe flood and drought in the Changjiang–Huaihe river basin. Adv Atmos Sci 20:540–553

Yang J, Wang B, Wang B et al (2010) Biweekly and 21–30-day variations of the subtropical summer monsoon rainfall over the lower reach of the Yangtze River basin. J Clim 23:1146–1159

Yang SY, Wu BY, Zhang RH et al (2013) The zonal propagating characteristics of low-frequency oscillation over the Eurasian mid-high latitude in boreal summer. Sci China Earth Sci. https://doi.org/10.1007/s11430-012-4576-z

Yang J, Bao Q, Gong DY, Wang B (2014) Distinct quasi-biweekly variations of the subtropical East Asian monsoon during early and late summers. Clim Dyn 42:1469–1486

Yatagai A et al (2012) APHRODITE: constructing a long-term daily gridded precipitation dataset for Asia based on a dense network of rain gauges. Bull Am Meteorol Soc 93:1401–1415

Zhang L, Wang B, Zeng Q (2009) Impacts of the Madden–Julian oscillation on summer rainfall in Southeast China. J Clim 22:201–216

Zhao C, Li T, Zhou T (2013) Precursor signals and processes associated with MJO initiation over the tropical Indian Ocean. J Clim 26:291–307